

Growth of High-Crystalline, Single-Layer Hexagonal Boron Nitride on Recyclable Platinum Foil

Gwangwoo Kim,[†] A-Rang Jang,^{†,‡,§,⊥} Hu Young Jeong,[§] Zonghoon Lee,^{||} Dae Joon Kang,[⊥] and Hyeon Suk Shin*,^{†,‡}

[†]Interdisciplinary School of Green Energy, Low Dimensional Carbon Materials Center, KIER-UNIST Advanced Center for Energy,

[‡]Institute of Nano Bio-science and Chemical Engineering, [§]UNIST Central Research Facilities (UCRF), ^{||}Department of Mechanical and Advanced Materials Engineering, Ulsan National Institute of Science and Technology (UNIST), UNIST-gil 50, Ulsan 689-805, Korea

[⊥]BK21 Physics Research Division, Department of Energy Science, SKKU Advanced Institute of Nanotechnology, Sungkyunkwan University, Suwon 440-746, Korea

S Supporting Information

ABSTRACT: Hexagonal boron nitride (h-BN) is gaining significant attention as a two-dimensional dielectric material, along with graphene and other such materials. Herein, we demonstrate the growth of highly crystalline, single-layer h-BN on Pt foil through a low-pressure chemical vapor deposition method that allowed h-BN to be grown over a wide area ($8 \times 25 \text{ mm}^2$). An electrochemical bubbling-based method was used to transfer the grown h-BN layer from the Pt foil onto an arbitrary substrate. This allowed the Pt foil, which was not consumed during the process, to be recycled repeatedly. The UV-visible absorption spectrum of the single-layer h-BN suggested an optical band gap of 6.06 eV, while a high-resolution transmission electron microscopy image of the same showed the presence of distinct hexagonal arrays of B and N atoms, which were indicative of the highly crystalline nature and single-atom thickness of the h-BN layer. This method of growing single-layer h-BN over large areas was also compatible with use of a sapphire substrate.

KEYWORDS: Hexagonal boron nitride, single layer, chemical vapor deposition, ammonia borane, platinum foil



Hexagonal boron nitride (h-BN), which has a two-dimensional (2D) strong sp^2 covalent bond-containing honeycomb structure that is similar to that of graphene,^{1–3} has attracted much attention because of its high mechanical strength and thermal conductivity.^{4–6} However, graphene exhibits semimetallic properties and has a zero band gap, while h-BN is an insulator with a direct band gap of 5–6 eV. This is attributable to the partially ionic character of the B–N bonds.^{7–11} In addition, in contrast to graphene h-BN is known to be chemically stable in air at temperatures as high as 1000 °C.^{12,13} Highly purified h-BN exhibits intense excitonic luminescence bands for wavelengths ranging from 215 to 227 nm, which are sufficiently strong to cause stimulated emission. Therefore, high-quality h-BN is a promising material for deep UV optoelectronic devices.¹⁴

Single-layer h-BN has been grown on single-crystal transition metals such as Au(111), Ru(001), Rh(111), and Pt(111) in ultrahigh vacuum (UHV) chemical vapor deposition (CVD) systems by introducing a borazine precursor.^{15–19} However, it is extremely difficult to grow and characterize single-layer h-BN and to transfer it onto other substrates, owing to the complex nature of the UHV CVD systems used. Along with the recent progress made in research on graphene, attempts have also been made to grow h-BN on Cu and Ni foils using atmospheric pressure CVD (APCVD) or low-pressure CVD (LPCVD)

methods and then transfer it onto other substrates via widely used etching processes.^{20–25} During these growth processes, h-BN has been known to exhibit different behaviors, depending on the precursor used. Borazine as a precursor induced growth of h-BN in multilayer form with the layers being between 5 and 50 nm in thickness.^{20,21} On the other hand, the use of a mixture of ammonia and diborane as the precursor suggested that the thickness of the grown h-BN layers could be controlled by changing the growth temperature and period; however, it was hard to obtain uniform single layers of h-BN because the growth rate during the process was high.²² The growth rate of h-BN can be decreased by using a powdered precursor such as ammonia borane. Indeed, it was reported that by using ammonia borane as the precursor, it was possible to grow single-layer h-BN on Cu foil within 40 min, with multiple layers being formed on some sites. It was also noticed that the density of these multiple layers increased with an increase in the growth period.²³

Herein, we report the growth of a high-quality single-layer h-BN over a large area via a simple LPCVD method. This growth

Received: February 12, 2013

Revised: March 21, 2013

Published: March 25, 2013



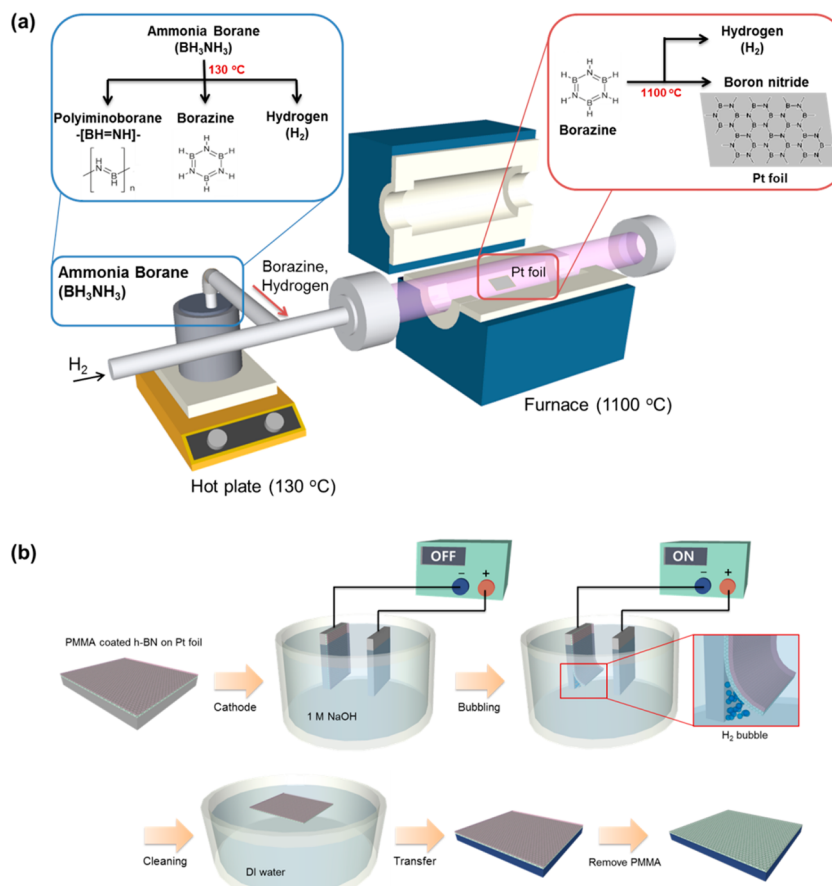


Figure 1. Schematic diagrams of the (a) LPCVD system used for h-BN growth and (b) electrochemical bubbling-based method used to transfer the h-BN layer.

was achieved by employing Pt foil and ammonia borane as the substrate and precursor, respectively. The single layer of h-BN grown on Pt foil could be successfully transferred onto an arbitrary substrate via an electrochemical bubbling-based method. This method of transferring h-BN has numerous advantages: it is rapid, allows for the recycling of the Pt foil, and does not result in Pt residues. High-resolution transmission electron microscopy (HRTEM) images showed clearly that the layer of h-BN comprised hexagonal arrays of B and N atoms, indicating the highly crystalline and single-layer nature of the grown h-BN.

Figure 1a shows a schematic of the LPCVD system used for growing single-layer h-BN. Ammonia borane ($\text{NH}_3\text{--BH}_3$) was used as the precursor because it is stable under ambient conditions. Borazine is moisture sensitive and can be hydrolyzed to boric acid, ammonia, and hydrogen.²⁶ To grow single-layer h-BN on Pt foil, the temperature within the LPCVD system was set to 1100 °C, and the precursor, ammonia borane, was heated to 130 °C, since it decomposes into hydrogen, polyiminoborane (BHNH ; solid), and borazine ($(\text{HBNH})_3$; gas) at this temperature.^{27,28} The produced borazine gas was made to diffuse from the source bottle into the furnace, where it was adsorbed onto the Pt foil. Single-layer h-BN was thus formed from borazine via thermal decomposition as shown in Figure 1a. Because of the weak bonding of the borazine molecules with the grown h-BN layer at the growth temperature, any precursor molecules that were adsorbed onto the grown layer were rapidly desorbed back into the gas phase.^{18,19} The growing h-BN film essentially

constituted an inert blanket that progressively covered an increasingly larger fraction of the Pt foil surface during the growth process, resulting in the eventual self-termination of the growth of the layer, with it being one atom thick. Thus, uniform, single-layer h-BN could be grown on Pt foil without multiple layers being formed, regardless of the duration of the growth process. In addition, we could also grow single-layer h-BN over the entire surface of a larger-sized piece of Pt foil that had dimensions of 8 × 25 mm². This suggested that larger-sized layers of h-BN could be grown, depending on the size of the Pt foil piece used as the substrate.

Pt foil is an expensive and chemically inert material. Thus, the commonly used etching-based transfer method for Cu and Ni substrates is not suitable for the transfer of the h-BN layer grown on Pt foil. Recently, it was reported that a bubbling-based transfer method, which is an electrochemical delamination technique, could be used to do so instead.^{29,30} We were able to use this bubbling-based transfer method to successfully transfer the h-BN layer grown on Pt foil onto arbitrary substrates in a manner that allowed the Pt foil to be recycled. Figure 1b shows a schematic of the bubbling-based transfer method, which is based on the electrolysis of water. After the growth of h-BN on Pt foil, PMMA was spin coated on the h-BN/Pt foil structure. Then, the structure comprising PMMA/h-BN/Pt foil was dipped into a 1 M aqueous solution of NaOH. While the PMMA/h-BN/Pt foil structure was used as the cathode, a piece of bare Pt foil was used as the anode. The application of a constant current for a few minutes caused the PMMA/h-BN layer to detach from the Pt foil because of the

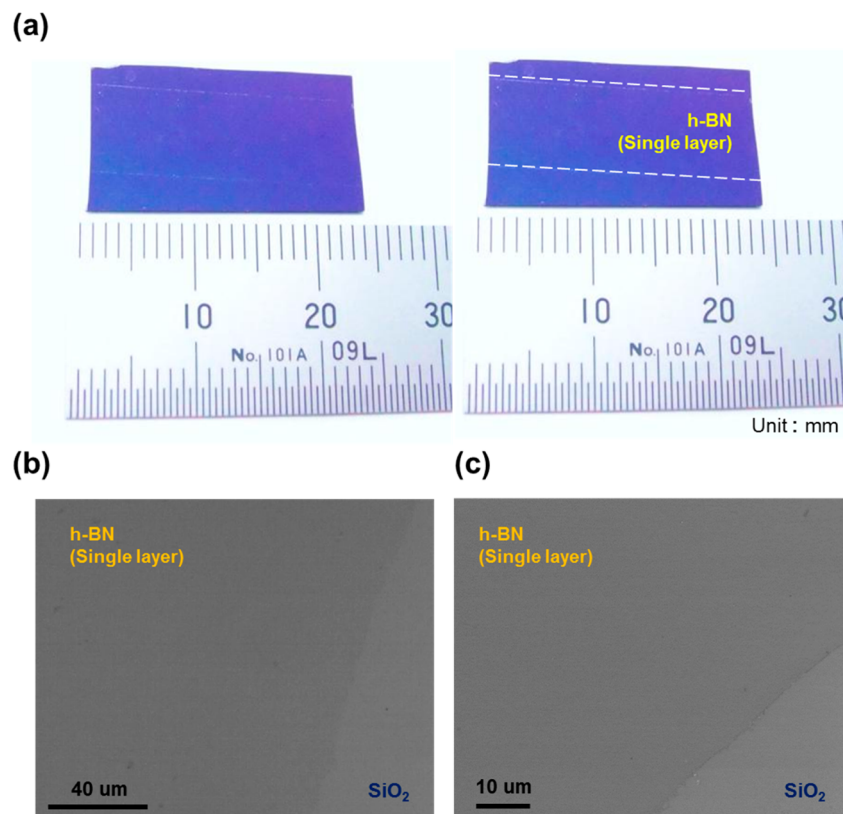


Figure 2. (a) Photograph of an h-BN layer transferred from Pt foil to a SiO₂/Si substrate. (b) Optical microscopy image of single-layer h-BN on a SiO₂/Si substrate, taken using 630 nm band-pass-filtered light. (c) SEM image of single-layer h-BN on a SiO₂/Si substrate.

formation of H₂ bubbles. The bubbling process could usually be completed in less than 5 min, a duration much smaller than that of the etching process using a etchant with Cu and Ni foils. Furthermore, the transferred h-BN layer was free of metal residues, which is an advantage of this transfer process. After the completion of the transfer process, the PMMA/h-BN layer was washed with deionized (DI) water to remove any remaining NaOH and transferred onto a target substrate. Finally, we removed the PMMA with acetone to obtain high-quality, single-layer h-BN. It should be noted that the Pt foil used in the growth of h-BN was recyclable since Pt was not consumed during the process.

It is hard to observe single-layer h-BN on a SiO₂(300 nm)/Si substrate using an optical microscope under a white light source because its optical contrast is less than 1.5%.³¹ Figure 2a shows an optical image of single-layer h-BN under a white light source. The h-BN region is barely distinguishable without residues at its edges. The contrast of a layer of BN on a SiO₂(300 nm)/Si substrate changes with the wavelength of the incident light.³¹ BN is darker than the substrate at wavelengths longer than ~530 nm and brighter at shorter ones with the optical contrast of single-layer h-BN on a SiO₂(300 nm)/Si substrate being the highest at 590 nm. Single-layer h-BN could be noticed more clearly under a light source with a 630 nm band-pass filter than was the case under a white-light source alone. Figure 2b shows an optical microscopy image of single-layer h-BN under a light source with a 630 nm band-pass filter. (See Supporting Information Figure S1 for the differences in the optical contrasts of h-BN under white-light sources with 425, 520, and 630 nm band-pass filters.) In contrast to optical microscopy, scanning electron microscopy (SEM) allowed us to easily identify an h-BN layer on a SiO₂/Si substrate (Figure

2c). The thickness of an h-BN layer transferred onto a SiO₂/Si substrate could be determined using atomic force microscopy (AFM). Figure 3a shows an AFM image of a layer of h-BN transferred onto a SiO₂/Si substrate, with the thickness of the layer, which was less than 0.48 nm, indicated in the image. This value was consistent with that reported previously for single-layer h-BN.²³ Note that the thicknesses of the h-BN layers grown on Pt foil using different growth periods (1–30 min) were all less than 0.48 nm, indicating that only single-layer h-BN was grown in all the cases (See Supporting Information Figure S2.)

Figure 3b shows the Raman spectrum of h-BN on a SiO₂/Si substrate, obtained using a 532 nm laser. A characteristic Raman peak of bulk, single-crystal h-BN was observed at 1366 cm⁻¹ and was attributable to the E_{2g} phonon mode.^{31,32} This peak shifts to ~1370 cm⁻¹ in the case of single-layer h-BN and to ~1364 cm⁻¹ for bilayer h-BN.³¹ In our study, the E_{2g} phonon mode for all h-BN layers grown using the various growth periods appeared at 1372 cm⁻¹, indicating that all the h-BN layers grown were monolayers (see Supporting Information Figure S3). The results of Raman spectroscopy were consistent with the AFM results.

The UV-visible absorption spectrum of single-layer h-BN was determined with the h-BN film exhibiting almost zero absorbance in the visible-light range and abrupt absorption in the UV region. This suggested the presence of an optical band gap (OBG), which was calculated using the formula for a direct band semiconductor⁷ and determined to be 6.06 eV, as shown in Figure 3d. This value was consistent with that predicted by theoretical calculations (6.0 eV).³³ X-ray photoemission spectroscopy (XPS) was performed on the as-grown single layer of h-BN to check for the presence of the elements B and

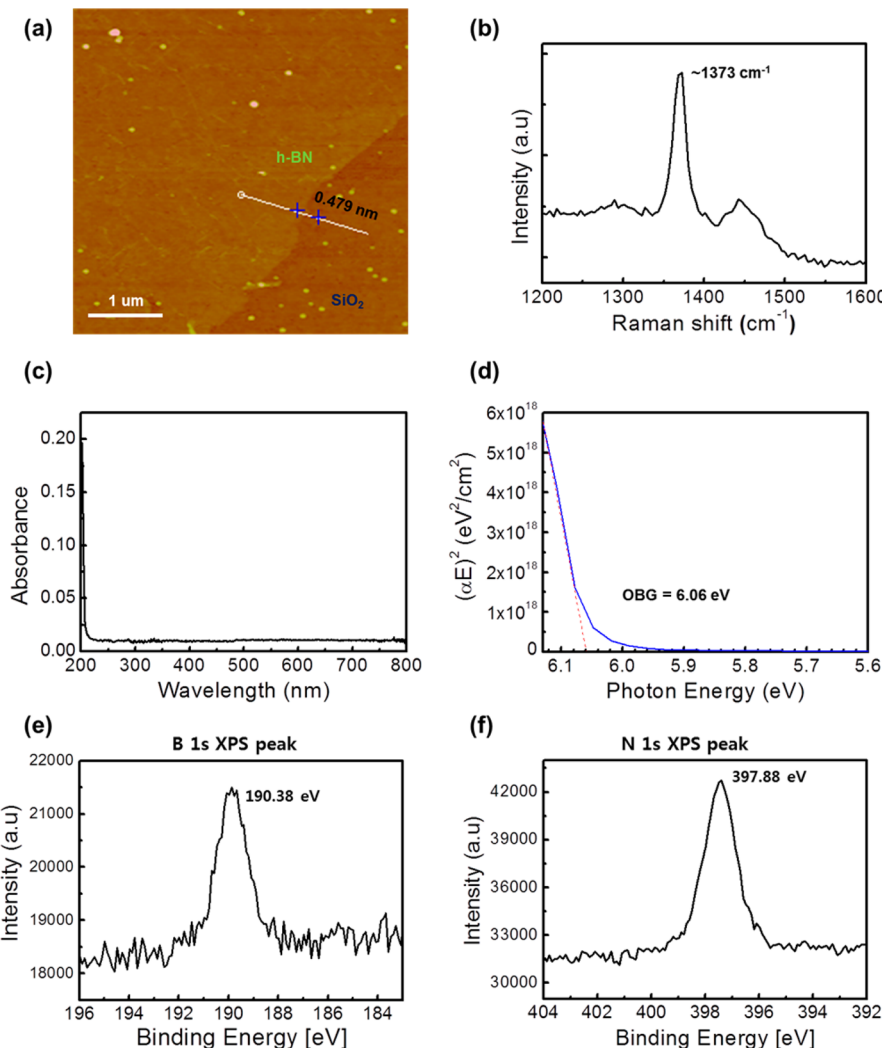


Figure 3. (a) AFM image of single-layer h-BN on a SiO_2/Si substrate. (b) Raman spectrum of single-layer h-BN on a SiO_2/Si substrate. (c) UV-visible absorption spectrum and (d) optical band gap analysis of single-layer h-BN on a quartz substrate. XPS spectra of h-BN on Pt foil: (e) B1s spectrum and (f) N1s spectrum.

N and to determine their elemental ratios. The binding energies for the B 1s and N 1s peaks, determined from the XPS spectra, were 190.38 eV (Figure 3e) and 397.88 eV (Figure 3f), respectively. These values matched with those previously reported for h-BN.^{20,22} The ratio of B and N atom % in single-layer h-BN, calculated from the XPS results, was 1:1.03.

Figure 4a shows a low-magnification bright-field TEM image of the freestanding h-BN film after it was transferred onto a hole with 2 μm in diameter in Au quantifoil TEM grid. The h-BN film covered the entire mesh well without broken regions and ripples. The selective area electron diffraction pattern in Figure 4b clearly indicates a set of hexagonal diffraction spots matched well with the (10 $\bar{1}\bar{0}$) index of single-layer h-BN. To directly observe the atomic structure of single-layer h-BN, we used a Cs aberration-corrected electron microscopy operated at 80 kV. We matched boron and nitrogen atom sites in the h-BN lattice, as illustrated in Figure 4c, since boron vacancies are first generated at 80 keV, followed by the removal of the neighboring nitrogen atoms that surrounded the point defects, owing to the difference in the knock-on damage thresholds of the boron (74 keV) and nitrogen (84 keV) atoms in a BN sheet.³⁴ The HRTEM image in Supporting Information Figure S4 was used for identifying the B and N atoms by the presence

of a single boron vacancy and an expanded large triangular defect. Electron energy loss spectroscopy (EELS) was qualitatively carried out for elemental analysis of the h-BN film. Figure 4d represents an EELS spectrum with two visible edges corresponding to the characteristic K-shell ionization edges of B and N, respectively.³⁵ In addition, the characteristic π^* and σ^* energy loss peaks at the boron K edge prove that h-BN has sp^2 hybridization bonds. Furthermore, it was found from dark-field TEM images that the grain size of h-BN reaches to a few micrometer range (see Supporting Information Figure S5 and S6). Details on the grain size and grain boundaries of h-BN are under study.

The quality of the h-BN layer was estimated on the basis of its resistance. It was previously reported that current can flow through the layer if the carbon is doped into h-BN.^{36,37} The electrical characteristics of the h-BN layer were determined using the four-point probe technique. Figure 5a shows an optical image of the four devices fabricated on a single layer of h-BN with the channel length and width being 1 and 5 μm , respectively. The $I-V$ curve in Figure 5b shows that no current flowed through the devices. The $I-V$ curves of the other devices were same as that in Figure 5b. Thus, it was determined

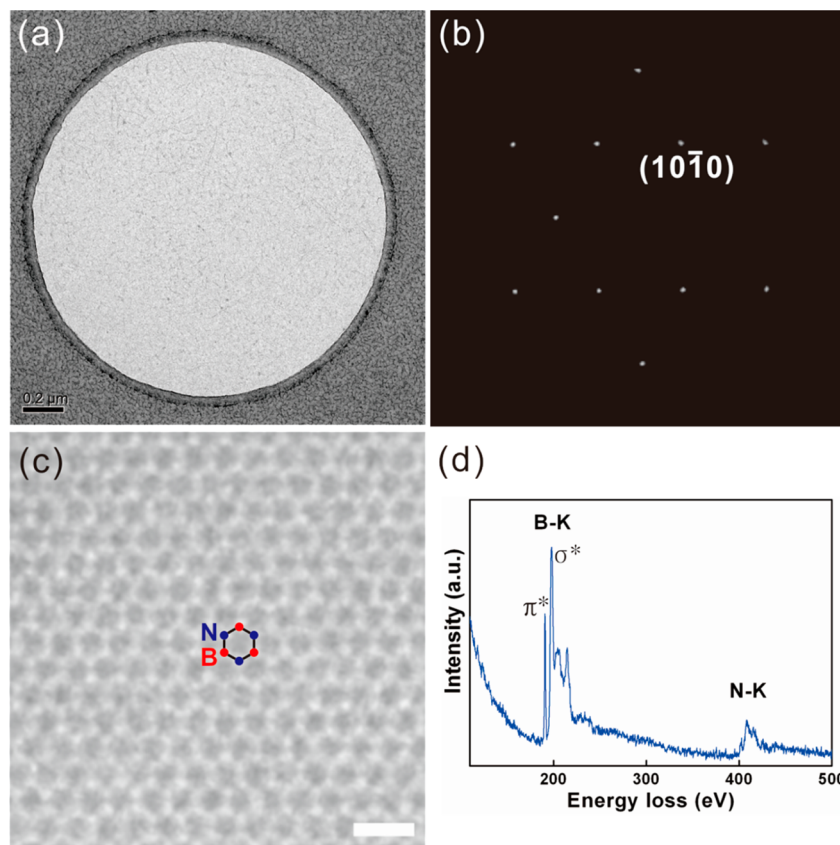


Figure 4. (a) A low-magnification TEM image of single-layer h-BN. (b) The corresponding diffraction pattern of single-layer h-BN showing a set of hexagonal patterns from single layer h-BN. (c) Atomic-resolution TEM image of single-layer h-BN (scale bar: 1 nm). (d) EELS spectrum of single-layer h-BN.

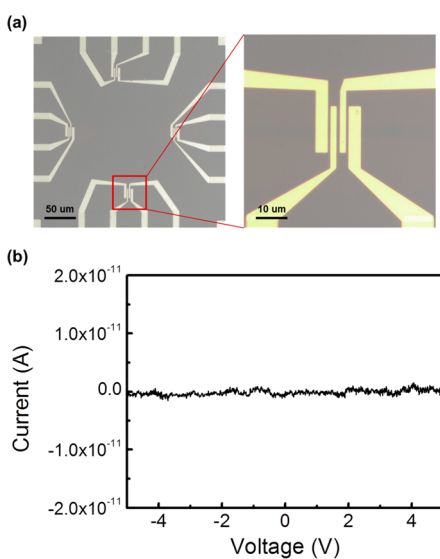


Figure 5. (a) Optical microscopy image of the four devices fabricated on single-layer h-BN for the four-point probe technique. (b) I – V curve of one of the single-layer h-BN devices, indicating the highly insulating nature of single-layer h-BN.

that the h-BN layer exhibited excellent insulating properties, which were indicative of its high quality.

As can be seen from Supporting Information Figure S7, there was no change in the quality of the h-BN layers grown even when the Pt foil was recycled and used to grow single-layer h-BN a 100 times. This showed that the Pt foil could be used

repeatedly as previously mentioned. Therefore, in contrast to Cu and Ni foils, Pt foil has numerous advantages. It allows for the synthesis of highly crystalline, single-layer h-BN with sufficient reproducibility while being recyclable. In addition, the formed single layer of h-BN could be transferred through a rapid bubbling-based method. Furthermore, this growth method was not limited to the use of Pt foil. Using this method, single-layer h-BN could also be grown on a sapphire substrate, as shown in Supporting Information Figure S8. Even though sapphire substrates do not allow for the grown layers to be readily transferred onto other substrates, they have great potential for use in optoelectronic devices such as deep UV light emitters and as oxidation resistance layers.

In summary, we were able to synthesize high-quality, single-layer h-BN on Pt foil over a large area using an LPCVD method. The h-BN film grown on Pt foil could be transferred onto a SiO₂/Si substrate by using the electrochemical bubbling-based method. The Pt foil could be used repeatedly, with the quality of the grown h-BN layers remaining unchanged even after 100 growth cycles. More importantly, the HRTEM results showed clearly the presence of hexagonal arrays of B and N atoms, indicating that the h-BN layer was highly crystalline and single-atom thick. The UV-visible absorption spectrum of single-layer h-BN revealed an optical band gap of 6.06 eV. The h-BN film also exhibited excellent insulating properties, suggesting that it can be used as a dielectric layer. This method provides a wide range of advantages in that it allows for the synthesis of highly crystalline, single-layer h-BN with sufficient reproducibility, with the Pt foil used during the process being recyclable. Further, the grown h-BN film could be transferred

to other substrates through the rapid bubbling-based transfer method.

■ ASSOCIATED CONTENT

Supporting Information

Detailed description of experimental details and additional information for optical microscope (OM) images of h-BN at different wavelengths, Raman and AFM results of h-BN with various growth periods. OM, SEM, AFM, and Raman results of single-layer h-BN on fresh Pt foil and 100 times recycled Pt foil. This material is available free of charge via the Internet at <http://pubs.acs.org>.

■ AUTHOR INFORMATION

Corresponding Author

*E-mail: shin@unist.ac.kr.

Author Contributions

G.K. and A.-R.J. contributed equally. The manuscript was written through contributions of all authors. All authors have given approval to the final version of the manuscript.

Notes

The authors declare no competing financial interest.

■ ACKNOWLEDGMENTS

This work was supported by the Basic Science Research Program (2011-0013601), the Grant (Code No. 2011-0031630 and 2011-0032153) from the Center for Advanced Soft Electronics under the Global Frontier Research Program, and Nano Material Technology Development Program (2012M3A7B4049807) through the National Research Foundation funded by MEST of Korea.

■ REFERENCES

- (1) Corso, M.; Auwarter, W.; Muntwiler, M.; Tamai, A.; Greber, T.; Osterwalder, J. *Science* **2004**, *303*, 217–220.
- (2) Paine, R. T.; Narula, C. K. *Chem. Rev.* **1990**, *90*, 73–91.
- (3) Lee, C.; Li, Q.; Kalb, W.; Liu, X.-Z.; Berger, H.; Carpick, R. W.; Hone, J. *Science* **2010**, *328*, 76–80.
- (4) Zhi, C.; Bando, Y.; Tang, C.; Kuwahara, H.; Golberg, D. *Adv. Mater.* **2009**, *21*, 2889–2893.
- (5) Lipp, A.; Schwerz, K. A.; Hunold, K. *J. Eur. Ceram. Soc.* **1989**, *5*, 3–9.
- (6) Sevik, C.; Kinaci, A.; Haskins, J. B.; Cagin, T. *Phys. Rev. B* **2012**, *86*, 075403.
- (7) Yuzuriha, T. H.; Hess, D. W. *Thin Solid Films* **1986**, *140*, 199–207.
- (8) Zunger, A.; Katzir, A.; Halperin, A. *Phys. Rev. B* **1976**, *13*, 5560–5573.
- (9) Watanabe, K.; Taniguchi, T.; Kanda, H. *Nat. Mater.* **2004**, *3*, 404–409.
- (10) Golberg, D.; Bando, Y.; Huang, Y.; Terao, T.; Mitome, M.; Tang, Ch.; Zhi, C. *ACS Nano* **2010**, *4*, 2979–2993.
- (11) Pacile, D.; Meyer, J. C.; Girit, C. O.; Zettl, A. *Appl. Phys. Lett.* **2008**, *92*, 133107.
- (12) Motojima, S.; Tamura, Y.; Sugiyama, K. *Thin Solid Films* **1982**, *88*, 269–274.
- (13) Hao, X. P.; Cui, D. L.; Shi, G. X.; Yin, Y. Q.; Xu, X. G.; Jiang, M. H.; Xu, X. W.; Li, Y. P. *Mater. Lett.* **2001**, *51*, 509–513.
- (14) Watanabe, K.; Taniguchi, T.; Niiyama, T.; Miya, K.; Taniguchi, M. *Nat. Photonics* **2009**, *3*, 591–594.
- (15) Simonson, R. J.; Paffett, M. T.; Jones, M. E.; Koel, B. E. *Surf. Sci.* **1991**, *254*, 29–44.
- (16) Nagashima, A.; Tejima, N.; Gamou, Y.; Kawai, T.; Oshima, C. *Phys. Rev. Lett.* **1995**, *75*, 3918–3921.
- (17) Preobrajenski, A. B.; Vinogradov, A. S.; Ng, M. L.; Cavar, E.; Westerstrom, R.; Mikkelsen, A.; Lundgren, E.; Martensson, N. *Phys. Rev. B* **2007**, *75*, 245412.
- (18) Paffett, M. T.; Simonson, R. J.; Papin, P.; Paine, R. T. *Surf. Sci.* **1990**, *232*, 286–296.
- (19) Sutter, P.; Lahiri, J.; Albrecht, P.; Sutter, E. *ACS Nano* **2011**, *5*, 7303–7309.
- (20) Shi, Y.; Hamsen, C.; Jia, X.; Kim, K. K.; Reina, A.; Hofmann, M.; Allen, L. H.; Zhang, K.; Li, H.; Juang, Z.-Y.; Dresselhaus, M. S.; Li, L.-J.; Kong, J. *Nano Lett.* **2010**, *10*, 4134–4139.
- (21) Kim, K. K.; Hsu, A.; Jia, X.; Kim, S. M.; Shi, Y.; Dresselhaus, M.; Palacios, T.; Kong, J. *ACS Nano* **2012**, *6*, 8583–8590.
- (22) Ismach, A.; Chou, H.; Ferrer, D. A.; Wu, Y.; McDonnell, S.; Floresca, H. C.; Covacevich, A.; Pope, C.; Piner, R.; Kim, M. J.; Wallace, R. M.; Colombo, L.; Ruoff, R. S. *ACS Nano* **2012**, *6*, 6378–6385.
- (23) Kim, K. K.; Hsu, A.; Jia, X.; Kim, S. M.; Shi, Y.; Hofmann, M.; Nezich, D.; Rodriguez-Nieva, J. F.; Dresselhaus, M.; Palacios, T.; Kong, J. *Nano Lett.* **2012**, *12*, 161–166.
- (24) Song, L.; Ci, L.; Lu, H.; Sorokin, P. B.; Jin, C.; Ni, J.; Kvashnin, A. G.; Kvashnin, D. G.; Lou, J.; Yakobson, B. I.; Ajayan, P. M. *Nano Lett.* **2010**, *10*, 3209–3215.
- (25) Lee, K. H.; Shin, H.-J.; Lee, J.; Lee, I.-Y.; Kim, G.-H.; Choi, J.-Y.; Kim, S.-W. *Nano Lett.* **2012**, *12*, 714–718.
- (26) Wolf, G.; Baumann, J.; Baitalow, F.; Hoffmann, F. P. *Thermochim. Acta* **2000**, *343*, 19–25.
- (27) Baitalow, F.; Baumann, J.; Wolf, G.; Jaenicke-Robler, K.; Leitner, G. *Thermochim. Acta* **2002**, *391*, 159–168.
- (28) Frueh, S.; Kellett, R.; Mallery, C.; Molter, T.; Willis, W. S.; King'ondu, C.; Suib, S. L. *Inorg. Chem.* **2011**, *50*, 783–792.
- (29) Wang, Y.; Zheng, Y.; Xu, X.; Dubuisson, E.; Bao, Q.; Lu, J.; Loh, K. P. *ACS Nano* **2011**, *5*, 9927–9933.
- (30) Gao, L.; Ren, W.; Xu, H.; Jin, L.; Wang, Z.; Ma, T.; Ma, L.-P.; Zhang, Z.; Fu, Q.; Peng, L.-M.; Bao, X.; Cheng, H.-M. *Nat. Commun.* **2012**, *3*, 699.
- (31) Gorbachev, R. V.; Riaz, I.; Nair, R. R.; Jalil, R.; Britnell, L.; Belle, B. D.; Hill, E. W.; Novoselov, K. S.; Watanabe, K.; Taniguchi, T.; Geim, A. K.; Blake, P. *Small* **2011**, *7*, 465–468.
- (32) Arenal, R.; Ferrari, A. C.; Reich, S.; Wirtz, L.; Mevellec, J.-Y.; Lefrant, S.; Rubio, A.; Loiseau, A. *Nano Lett.* **2006**, *6*, 1821–1816.
- (33) Blasé, X.; Rubio, A.; Louie, S. G.; Cohen, M. L. *Phys. Rev. B* **1995**, *51*, 6868–6875.
- (34) Meyer, J. C.; Chuvalin, A.; Algara-Siller, G.; Biskupek, J.; Kaiser, U. *Nano Lett.* **2009**, *9*, 2683–2689.
- (35) Chopra, N. G.; Luyken, R. J.; Cherrey, K.; Crespi, V. H.; Cohen, M. L.; Louie, S. G.; Zettl, A. *Science* **1995**, *269*, 966–967.
- (36) Ci, L.; Song, L.; Jin, C.; Jariwala, D.; Wu, D.; Li, Y.; Srivastava, A.; Wang, Z. F.; Storr, K.; Balicas, L.; Liu, Feng.; Ajayan, P. M. *Nat. Mater.* **2010**, *9*, 430–435.
- (37) Wang, X.; Zhi, C.; Li, L.; Zeng, H.; Li, C.; Mitome, M.; Golberg, D.; Bando, Y. *Adv. Mater.* **2011**, *23*, 4072–7076.